euronoise

Characteristics of sound pressure field focused by an acoustic aplanat lens

Toshiaki Nakamura[a], Yuji Sato[b], Ayano Miyazaki[a] and Kazuyoshi Mori[a]

[a]National Defense Academy, 1-10-20 Hashirimizu, 239-8686 Yokosuka, Japan
[b]Tsukuba Univ., Tsukuba Science City, 305-8573 Ibaraki, Japan
toshiaki@nda.ac.jp

In this paper, we describe the characteristics of an acoustic aplanat lens which can eliminate both spherical and coma aberrations. A singlet aplanat lens was designed using a ray theory in paraxial area. Sound pressure fields of the bi-concave aplanat lens with 160 mm in diameter for the frequency of 500 kHz were evaluated by a three-dimensional finite difference time domain (3-D FDTD) method. The calculated characteristics were compared with the experimental result in a water tank. As a result, the on-axis sound pressure distributions around the focus agreed well each other except the difference of the focus positions between them. And the beam patterns at the focus agreed approximately for experimental and calculated results. It was found that the 3D-FDTD method was able to simulate the lens characteristics at normal incidence and oblique incidence within 10 degrees.

1 Introduction

An acoustic lens is a useful devise which can make high sound pressure at a small region to obtain a high resolution acoustic image and many researchers have been studying acoustic lenses from 1970s [1]. Recently, the underwater imaging sonar system using an acoustic lens is receiving attention again because it does not need to require a complex beam-forming circuit. The shapes of a singlet lens used for this type of sonar were a spherical [2] or an aspherical [3] lenses, but any lens couldn't focus completely because of lens aberrations.

In the field of optics, absolutely aplanatic lens which can remove a spherical aberration and a coma aberration in paraxial area was designed by using a numerical ray tracing method [4] and applied to optical disk system [5]. In this report, we designed two types of absolutely aplanatic acoustic lens by applying this method to underwater acoustic lens [6-8].

We made a bi-concave aplanatic lens with the diameter of 160 mm by an acrylic resin and evaluated the focusing characteristics by the 3-D FDTD method and compared with the experimental results with the frequency of 500 kHz in a water tank.

2 Design of aplanatic lens

An acoustic ray travels into a lens as shown in Fig. 1. In paraxial area, the principle of equal optical path must be satisfied to be free from a spherical aberration, which means the central optical path length and any other optical path length are equal.

When Abbe's sine condition is satisfied under the condition without a spherical aberration, a coma aberration is removed. The principle of equal optical path and Abbe's sine condition are respectively,

$$nd + f_b = a + nb + c\,, \tag{1}$$

$$\sin u_2 = \frac{h}{f}\,, \tag{2}$$

where n is the index of refraction, d is the thickness of lens, f_b is the length of the back focus, a, b, c are the path length of before-incidence, in the lens and after-projection, u_2 is the secondary angle of the refraction, h is the height of incidence, and f is the focal length. But $a = 0$ at the center of the first surface of the lens. At a triangle including b, a cosine formula and a sine formula are

$$b^2 = q^2 + (f-c)^2 - 2q(f-c)\cos u_2\,, \tag{3}$$

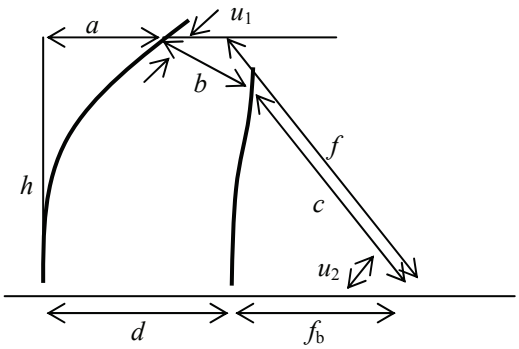

Fig. 1 Geometry of an aplanatic lens.

$$q = d + f_b - f\cos u_2 - a\,, \tag{4}$$

$$\frac{f-c}{\sin u_1} = \frac{b}{\sin u_2}\,, \tag{5}$$

where u_1 is the primary angle of the refraction.

It is possible to design the shape of a lens to solve formulas (1) to (5), but it's very difficult to solve these formulas analytically, so the lens surface is segmentalized into the discrete domains for numerical calculation according to Yoshida's method [4].

We show the designed lens shapes and the paths of rays refracted by four types of lenses which are a bi-concave spherical lens a plano-elliptic acoustic lens, a bi-convex aplanatic acoustic lens and a bi-concave aplanatic acoustic lens.

Results of the ray tracing method at 0° and 10° incidence are shown in Figs. 2 (a) - (d). Fig. 2 (a) shows a bi-concave spherical acoustic lens with the refractive index n = 0.56 corresponded with acrylic resin, the aperture of lens l = 160 mm, the thickness of lens d = 5 mm and the focal length f = 150 mm, Fig. 2 (b) shows a plano-elliptic acoustic lens with n = 0.56, l = 160 mm, d = 5 mm and f = 170 mm, Fig. 2 (c) shows a bi-convex aplanatic acoustic lens with n = 1.5 corresponded with silicon rubber, l = 100 mm, d = 30 mm, the central radius of curvature of the first surface r = 87.5 mm and f = 150 mm and Fig. 2 (d) shows a bi-concave aplanatic acoustic lens with n = 0.56, l = 160 mm, d = 5 mm, r = 284.6 mm and f = 150 mm. The size of the bi-convex aplanatic acoustic lens shown in Fig. 2 (c) is smaller than the others to decrease the attenuation of lens. If it has a large aperture, the lens must become thick and the attenuation gets larger.

As the bi-concave spherical acoustic lens does not satisfy the principle of equal optical path, it can't remove a spherical aberration and makes large caustic surfaces in the cases of 0° and 10° incidence as shown in Fig. 2 (a). The plano-elliptic lens can concentrate sound ray at the focal

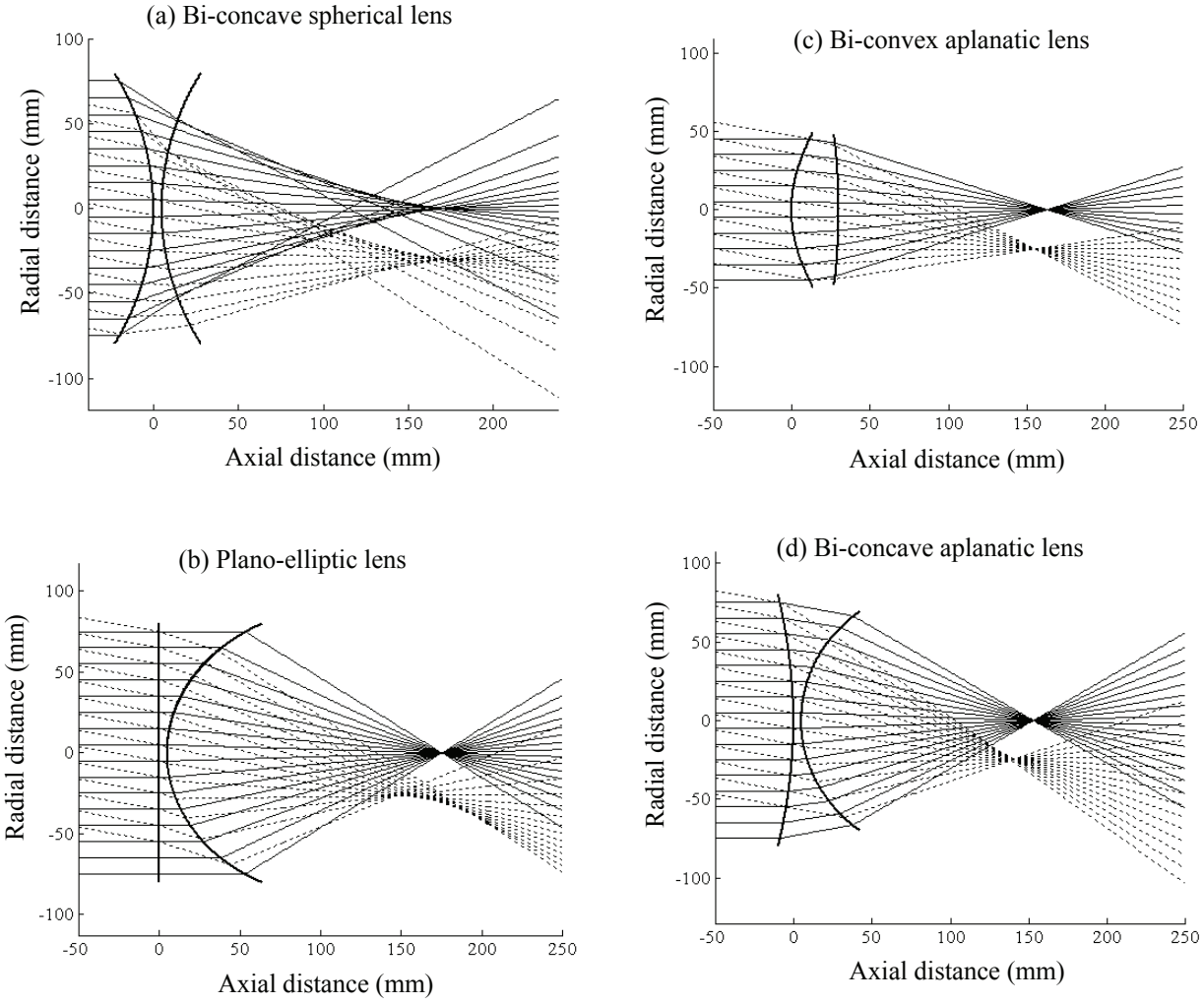

Fig. 2 Path diagrams of four types of lenses for 0° (solid lines) and 10° (dotted lines) incidence.
(a) bi-concave spherical, (b) plano-elliptic, (c) bi-convex aplanatic and (d) bi-concave aplanatic lenses.

point of the axial distance x = 175 mm without a spherical satisfies the principle of equal optical path as shown in Fig. 2 (b). However, a coma aberration is not removed in the case of 10° incidence because it does not satisfy the Abbe's sine-condition.

The bi-convex and the bi-concave aplanatic acoustic lenses concentrate sound rays at the focal point of normal incidence whose axial distance x = 155 mm and they can remove spherical and coma aberrations as shown in Figs. 2 (c) and (d) because it satisfies both of the principle of equal optical path and the Abbe's sine-condition.

The focal point of 10° incidence makes an approach to the lens because of aberration of a field curvature. Although it needs two or more lenses to remove this aberration, it's a future problem.

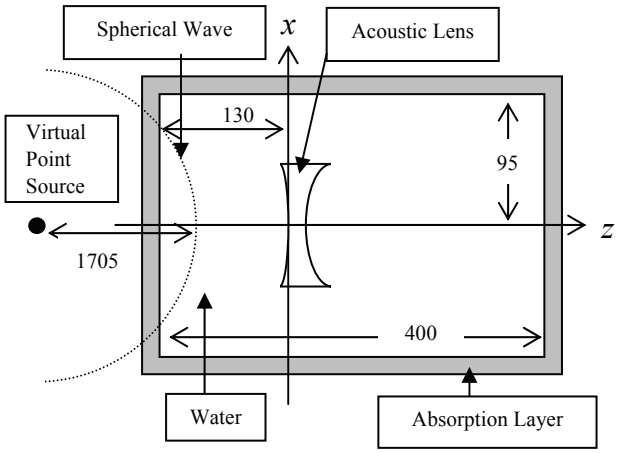

Fig. 3 Geometrical arrangement for 3D-FDTD method

3 3-D FDTD method

The focusing characteristics for the biconcave aplanat lens designed in the previous section were evaluated by using the 3D-FDTD method because a ray theory cannot evaluate the sound pressure level focused by a lens.

The 3D-FDTD is a method to obtain the time-step solution of a wave equation by the use of finite difference approximation of time and space to analyzing the sound pressure distribution [9]. It can calculate the waveforms at receivers, make snapshots, and model the parameters of experiment easily. However, it is difficult to perform the propagation analysis in a large-scale area because it takes very long time to calculate and a lot of memories are used.

The calculation area is enclosed by the absorption layer in order to simulate the propagation in a free space as shown in Fig. 3. The calculation time has been shortened by arranging many point sources on the sphere from the virtual sound source in the form of the concentric circle of 1,705 mm in radius. It enables to skip the time for propagation from a sound source to lens. The step size of the analysis was $\Delta x, y, z = 0.2$ mm in space domain and $\Delta t = 0.04$ μs in time domain. The range of the analysis was –95 mm to 95 mm along x and y axes, and –130 mm to 270 mm along z axis. Speed of sound and the density were assumed to be 2670 m/s and 1200 kg/m^3 respectively in the acoustic lens, 1500 m/s and 1000 kg/m^3 in the water and absorption layer. Attenuation was assumed $\gamma_2 = 0.0$ dB/ λ in water, $\gamma_2 = 0.5$ dB/λ in the lens, $\gamma_2 = 5.0$ dB/ λ in the absorption layer. The thickness of the absorption layer was assumed to be 10 mm. In addition, the first absorption boundary condition of Mur was applied to the absorption layer [10].

The biconcave acoustic lens used in the calculation and the experiment in the next section is made of acrylic resin and has both aspherical surfaces and a diameter of 160 mm as shown in Fig.4. The frequency impinging to the lens is 500 kHz.

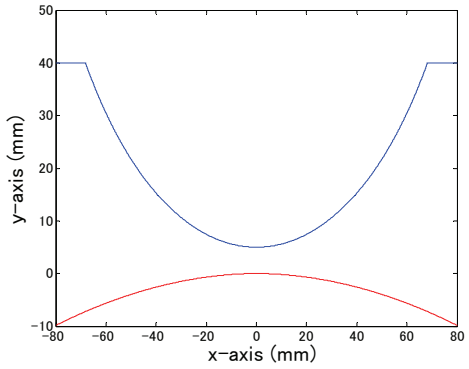

Fig. 4 Cross-section of bi-concave aplanatic lens with the diameter of 160 mm and the thickness at the center of 5 mm, made by acrylic resin (n=0.56).

4 Experiment in water tank

Experiments were conducted in a water tank with the size of 2 × 3 × 0.6 m filled with fresh water. Figure 5 shows the experimental setting in water tank. The projector used in this experiment has a diameter of 24 mm and a 3 dB beam width of 10° at 500 kHz.

The lens is suspended at the half-depth of the water tank from a shaft which can rotate for the measurements of oblique incidence. The distance from the projector to the lens is approximately 1.8 m. A hydrophone installed on an x-y-z stage controlled by a computer is set behind the lens. The diameter of the hydrophone sensor is 4 mm and has a flat frequency response of up to 800 kHz. The accuracy of the recursive positioning of the hydrophone is ±0.1 mm. The projector radiates a burst pulse of 5 cycles of a sinusoidal wave of 500 kHz. The pulse width is 10 μs.

The reflected waves at the surface and bottom of the water tank can be separated from the transmitted wave through the lens on the time axis due to a pass difference of 60 μs between them, and they do not affect the measurement of the transmitted wave. The reflection from the wall of the water tank is considerably delayed in comparison with the reflected waves. Sound pulse passing through the lens is received by the hydrophone. The received signal is amplified, filtered, and converted to digital data for a sampling time of 200 ns and stored in a computer. The sound field focused by the acoustic lens is measured by moving the hydrophone along and across the x-axis using the x-y-z-stage in the water tank.

We measured the characteristics on the two lines which are on-axis characteristics and beam patterns. The former is the sound pressure distribution along the line though the center of lens and the focus. The latter is the sound pressure distribution along the parallel line to the lens across the focus.

Measurements were repeated ten times on the same point to reduce the ambient noise level and averaged by a cyclic summation on the time domain. The sound pressure level on that point was obtained by the rms value of the averaged wave.

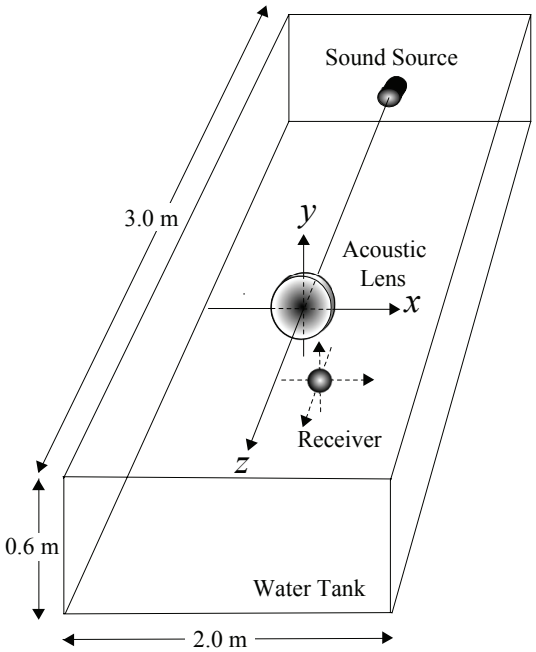

Fig. 5 Experimental setting in water tank using the frequency of 500 kHz

5 Results

The obtained sound pressure distribution by 3D-FDTD method and experiment in water tank are shown in Figs. 6 and 7. The results of the 3D-FDTD method are shown by the squared sum on the time direction in a similar way to the experiment.

Figures 6 (a) and (b) show the experimental results (thick line) of the sound pressure distribution on axis at normal (0 degree) and oblique (10 degrees) incidence compared with the calculation result by the 3D-FDTD method (thin line) of aplanat lens. The ordinate shows a relative sound pressure normalized by each maximum value. The abscissa shows an axial distance from the lens.

The focus position by the 3D-FDTD method was located behind that of experiment at both cases of normal and oblique incidence. The difference between calculation and experiment was 26 mm approximately. The similar results

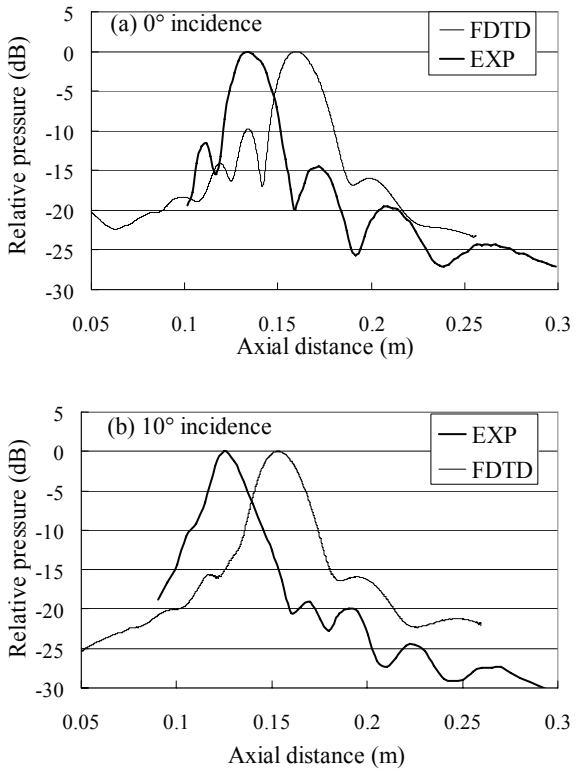

Fig. 6 On-axis characteristics of experimental results (thick line) and calculation results (thin line) for 0° incidence (a) and 10° incidence (b).

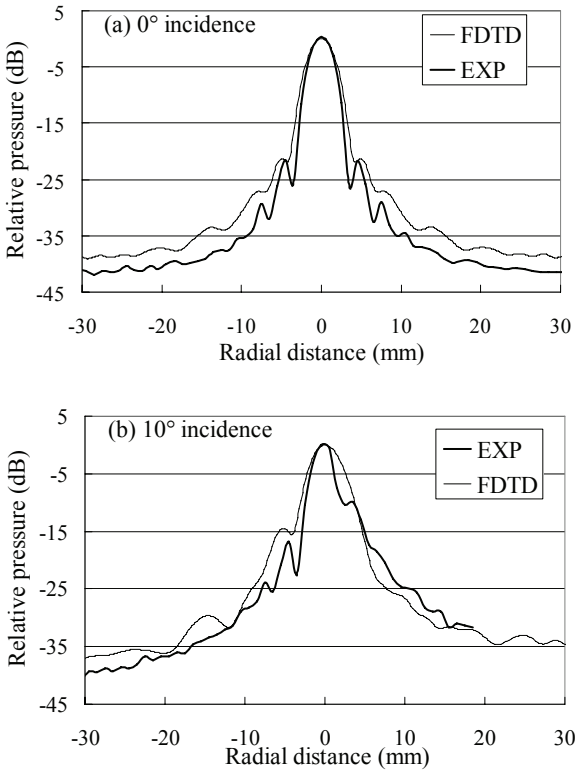

Fig. 7 Beam patterns at the focus of experimental results (thick line) and calculation results (thin line) for 0° incidence (a) and 10° incidence (b).

were obtained in the comparison with the 2D-FDTD method with the experiment in our previous report [8]. The reason of the difference is not clarified yet.

The dip before the focus of 3D-FDTD method was deeper than that of experimental result at normal incidence but the dips behind the focus of the experiment was deeper than that of the calculation. Calculation result attenuated smoothly without any dip behind the focus. The shapes around the focus agree well at the normal incidence as shown in Fig. 6 (a). In the case of the oblique incidence, the shape around the focus of experiment is sharper than that of calculation as shown in Fig. 6 (b).

Figures 7 (a) and (b) are the beam patterns at focus position comparing the experimental result (thick line) with the calculation result (thin line) by the 3D-FDTD method at normal (0 degree) and oblique (10 degrees) incidence. The ordinate shows a relative sound pressure normalized by each maximum value. The abscissa shows the radial distance from the peak and the peak position is set to zero in each result of experiment and calculation in order to compare the shapes of each beam pattern.

The calculation result by the 3D-FDTD method agreed well with the experimental result in the vicinity of the maximum value and the first sidelobe level at the normal incidence as shown in Fig. 7 (a). In the case of the oblique incidence, the envelope curves agreed approximately but there are many side-lobes in the experimental result as shown in Fig. 7 (b). The slight difference between real lens and model lens may affect the results of the sound pressure distribution, especially in the case of oblique incidence.

6 Conclusion

Two types of absolutely aplanatic acoustic lenses satisfying the principle of equal optical path and the Abbe's sine-condition were designed by the numerical ray tracing method. It could be concluded that the bi-concave and the bi-convex aplanatic lenses have the superior characteristics at normal and oblique incidence in comparison with spherical and plano-elliptic lenses, because aplanatic lenses could concentrate the collimated sound rays to one point with no aberrations.

Next, the focusing characteristics of a bi-concave aplanatic lens made by acrylic resin were evaluated by the 3D-FDTD method and compared with the experimental result in a water tank. As a result, the on-axis sound pressure distributions around the focus agreed well each other except the difference of the focus positions between them.

Experimental result and calculation result agreed well for the beam pattern at normal incidence. The envelope curves in both results agreed approximately in the case of the oblique incidence of 10°. It was found that the 3D-FDTD method was able to simulate the lens performance at normal and oblique incidence within 10°.

It is a future problem on the more precise simulation in the case of oblique incidence. It is also a future problem that the difference of focal length between experiment and calculation by 3D-FDTD method should be analysed.

Acknowledgments

The authors would like to thank Dr. Y. Tanaka (Matsushita Electric Industry Co.) for his helpful discussion.

References

[1] D. L. Folds, "Status of Ultrasonic Lens Development," *Underwater Acoustics and Signal Processing*., (D. Reidel Publishing Company, 1981) p.263

[2] T. Nakamura, Y. Sato, T. Kamakura and T. Anada, "Sound Pressure Fields Focused using Biconcave Acoustic Lens for Normal Incidence", *Jpn. J. Appl. Phys.*, **43,** 3163-3168 (2004)

[3] A. Miyazaki, H. Isshiki, K. Mori, T. Nakamura, "Sound Pressure Field Focused by an Aspherical Biconcave Lens for Normal and Oblique Incidence", *Proc. WESPAC IX.*, CDROM p284, (2006)

[4] S. Yoshida, "Calculation Concerning Aspheric Aplanatic Lens with Exceptionally Large Aperture Ratio. III", *Tohoku Univ. Research Institute for Scientific Measurements*, **6**, 25-144 (1958) [in Japanese]

[5] Y. Tanaka, M. Yamagata, T. Sasano, "Lens Design for Aplanatic Singlet and Its Application to Optical Disk System", *Appl. Opt*., **27**, 720-726 (1998) [in Japanese]

[6] Y. Sato, A. Miyazaki, K. Mori, T. Nakamura, "Design of an Absolutely Aplanatic Acoustic Lens", *Jpn. J. Appl. Phys*., **46**, 4982-4989 (2007)

[7] T. Nakamura, Y. Sato, A. Miyazaki, K. Mori, T. Kamakura, "Characteristics of an Absolutely Aplanatic Acoustic Lens", *Proc. ICU 2007* (2008) (to be published)

[8] Y. Sato, A. Miyazaki, K. Mori, T. Nakamura, "Convergence Characteristics of an Acoustic Aplanatic Lens", *J. Marine Acoust. Soc. Jpn.*, **35** (2008) [in Japanese] (to be published)

[9] K. Mori, T. Nakamura, T. Yokoyama, A. Hasegawa, "3-D FDTD Analysis of Sound Field Focused by Biconcave Acoustic Lens for Normal Incidence," *Jpn. J. Appl. Phys*., **44**, 4696-4701 (2005)

[10] G. Mur, "Absorbing Boundary Conditions for the Finite-Difference Approximation of the Time-Domain Electromagnetic-Field Equation," *IEEE Trans. Electromagnetic compat*., EMC-23, 377-382 (1981)